The Langmuir-Hinshelwood Reaction between Oxygen and CO at Ir(111) Surfaces

J. Küppers and A. Plagge
Institut für Physikalische Chemie der Universität München, Munich, Germany

Z. Naturforsch. **34a**, 81–88 (1979); received June 1, 1978

Dedicated to Prof. G. M. Schwab on the occasion of his 80th birthday

The reaction of oxygen and CO to form CO_2 has been investigated using an Ir (111) surface as an acting catalyst. Both instationary and stationary reaction processes have been established via separate gas exposing techniques. The instationary reaction process, achieved from coadsorbed CO and O which per se is an LH reaction is found to be controlled by an apparent activation energy of 10.7 kcal/mole. The stationary reaction with both CO and O_2 continuously present in the gas phase has been simulated using a proper computer program, involving both LH and ER reaction steps. By comparison with experimental results, close agreement is found when ruling out any ER reaction step from the reaction path.

1. Introduction

The application of modern surface analytical methods has opened the possibility to study reactions at surfaces under well defined and continuously monitored conditions. Although a simple reaction proceeding at a well prepared single crystal surface is far less complex than the processes appearing at practical catalysts, the study at those small model surfaces is of great importance to get a close insight into the reaction steps controlling a catalytic reaction.

Especially the oxidation of CO has gained considerable interest in the recent past and has been investigated using several materials: Pd [1], Pt [2], Ir [3] and Ru [4].

From these studies it is generally accepted that a necessary step for the reaction is the dissociation of O_2 which occurs upon oxygen adsorption. On the other hand from stationary reaction rate measurements it was concluded that adsorbed CO acts as an inhibitor for the reaction, this leading to the conclusion that the reaction proceeds via

$$O_{ad} + CO_g \rightarrow CO_2$$

i.e. an Eley-Rideal (ER) reaction mechanism. Very recently there was shown using molecular-beam techniques [5], that this conclusion was wrong and the reaction procieds via

$$O_{ad} + CO_{ad} \rightarrow CO_2$$

i.e. a Langmuir-Hinshelwood mechanism, the ER reaction being definitely excluded. From a LEED/UPS/TDS-study this conclusion was confirmed [6]. The present study was performed using an Ir(111) surface as an acting catalyst. Both, instationary and stationary CO_2 formation was investigated. The latter results were compared with a computer simulation in which the reaction parameters evaluated from the instationary reaction measurements were included.

Support by the Deutsche Forschungsgemeinschaft through SFB 128 is gratefully acknowledged.

2. Experimental

The experiments have been carried out in an UHV system equipped with LEED, RFA-Auger spectroscopy and a quadrupole mass spectrometer for determination of the partial pressures during reactions. The sample was cut from a single crystal rod as a disk-shaped slice in the (111) direction and mounted to a specimen manipulator via spot welding it to W-wires which served also for heating of the sample. The temperature of the sample was measured using a Ni/NiCr thermocouple spotwelded to one sideface of the disk. Using additional cooling, temperatures down to 150 K could be achieved.

3. Results

3.1. Cleaning Procedure

The sample was cleaned by Ar^+-bombardment and prolonged heating at 900 K in 10^{-7} torr oxygen. After flashing the sample in vacuo up to ~ 1500 K, from AES no contaminants — carbon and oxygen turned out to be most important — could be detected. The LEED-pattern at this stage displayed a sharp 1×1 structure.

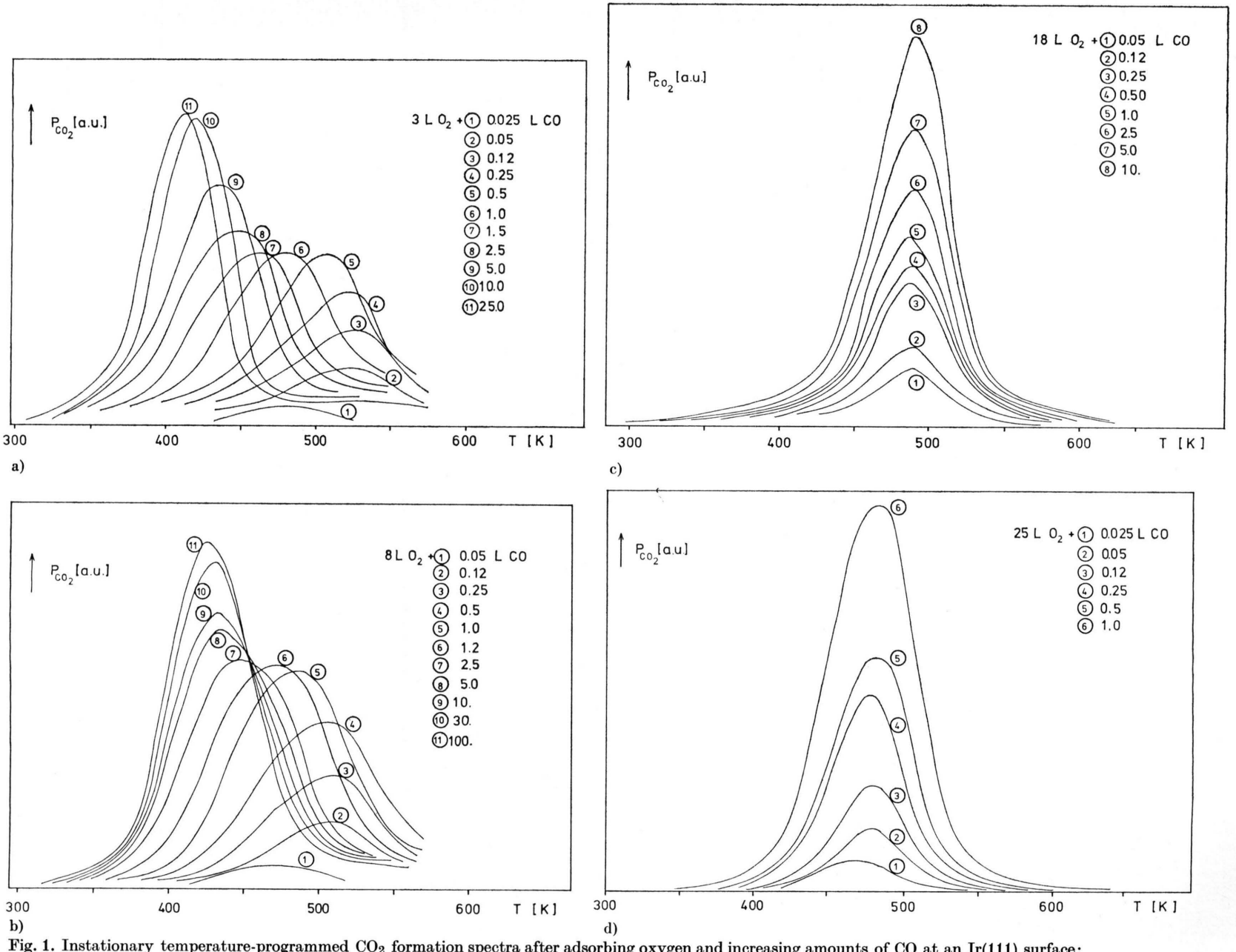

Fig. 1. Instationary temperature-programmed CO_2 formation spectra after adsorbing oxygen and increasing amounts of CO at an Ir(111) surface: a) 3 L O_2 preexposure, b) 8 L O_2 preexposure, c) 18 L O_2 preexposure, d) 25 L O_2 preexposure.

3.2. Adsorption Experiments

The results of oxygen and CO adsorption experiments have been published previously [3a] and will only be reported shortly. CO adsorbs with an initial sticking probability s near unity, the adsorption energy E_{ad} being 35 kcal/mole. With increasing coverage Θ, s and E_{ad} decrease slowly reaching $s(\Theta = 1/3) = 0.6$, $E_{ad}(\Theta = 1/3) = 33$ kcal/mole and $s(\Theta = 2/3) \leqq 0.05$, $E_{ad}(\Theta = 2/3) = 31$kcal/mole. Within this coverage range $0 \leqq \Theta \leqq 2/3$ from the LEED pattern a series of ordered adsorption structures is visible from which it can be concluded that the CO molecules at $\Theta = 1/3$ arrange themselfs in a hexagonal superlattice, the unit cell of which is uniaxially compressed upon increasing coverage. Oxygen is found to adsorb dissociatively with $s(\Theta \approx 0) = 0.02$, and $E_{ad}(\Theta \approx 0) = 65$ kcal/mole. With increasing coverage s increases slightly up to $s(\Theta = 0.2) \approx 0.07$, then dropping rapidly. At the total exposure of 22 L (1 L $\triangleq 10^{-6}$ torr · sec) the LEED pattern shows a 2×2 superstructure, the coverage at this stage being 0.25. Further exposure of oxygen results in a very slow oxygen uptake, indicating an extremely small sticking coefficient, similar to the results with other platinum metals.

3.3. Instationary Reaction

The experiments investigating the instationary reaction were performed using conditions from which obviously only a LH reaction path is possible. Initially oxygen is exposed to the surface followed by exposure of CO while the sample temperature was held at 300 K. By monitoring the CO_2 partial pressure it is seen, that no CO_2 is formed during this procedure. Then the sample is heated using a linear temperature increase: $T = T_0 + \beta t$. During heating the CO_2 partial pressure is recorded. A series of those desorption — better: reactive desorption — spectra is displayed in Figure 1. Three major characteristics can be identified appearing at different preadsorbed amounts of oxygen. With low oxygen coverages (Fig. 1a and b) the CO_2 formation curve shifts to lower temperatures upon increasing amounts of coadsorbed CO. At medium oxygen coverage (Fig. 1c) the maximum of the CO_2 formation rate appears at a constant temperature, whereas at high oxygen coverage (Fig. 1d) this maximum shifts slightly to higher temperature. Of course there is an increase of the total formed amount of CO_2 upon increasing the CO exposure seen with each oxygen exposure. Inspection of Fig. 1b shows that the shift of the CO_2 formation maximum is not continuous. Instead, at low and high CO coverages the maximum rate occurs at constant temperatures of 510 K and 430 K respectively, only with medium exposures of CO the peak shifts upon increasing CO exposure. Using those terms applied to thermal desorption spectroscopy the CO_2 formation in

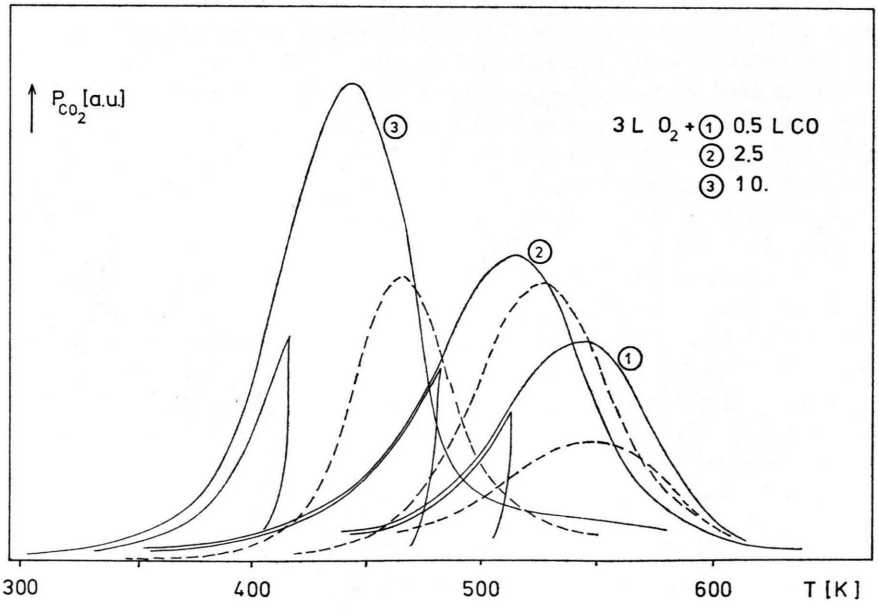

Fig. 2. Instationary CO_2 formation spectra after adsorbing oxygen and increasing amounts of CO at an Ir(111) surface: a) upper full curve: without interruption of the temperature rise, b) lower full curve: with interruption of the temperature rise, c) broken curve: after interruption of the temperature rise.

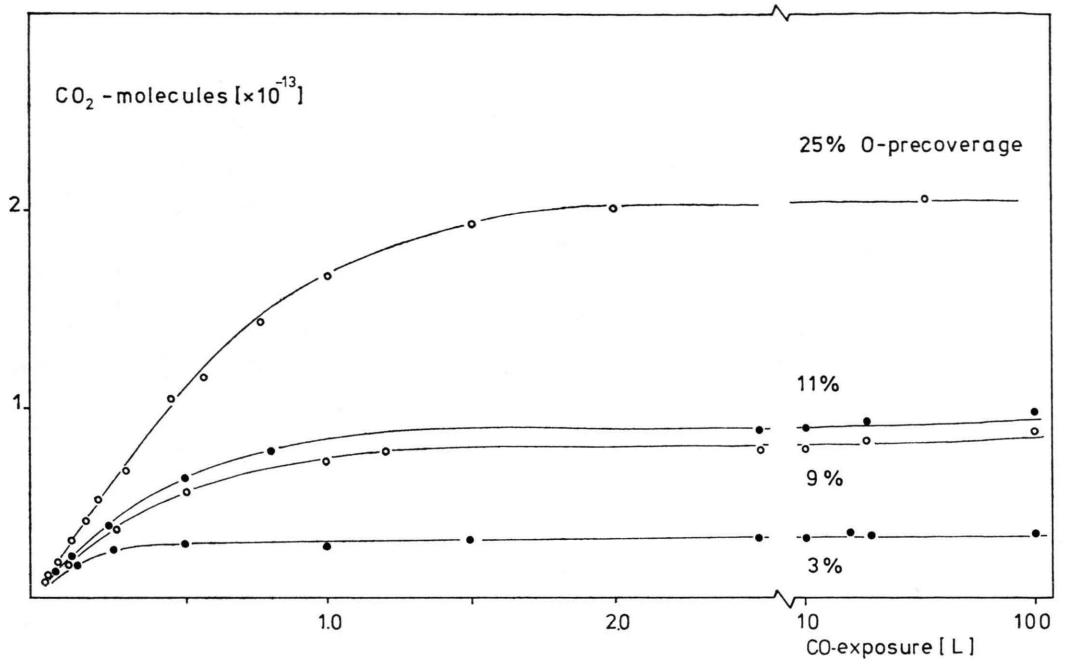

Fig. 3. Integrated CO_2 formation spectra measured with different oxygen coverages and increasing CO exposures.

Fig. 1 a, b seems to be of first order at low and high CO coverages and of second order at medium CO coverages. In order establish, that the shifts of the CO_2 peak maxima correlate only with a specific set of Θ_O, Θ_{CO} and are not caused by equilibration within the adlayer, experiments have been carried out in which the temperature sweep was stopped after a specific amount of CO_2 ($\sim 20\%$ of the total amount) has been desorbed. A typical example for these results is shown in Figure 2. The broken curves display the CO_2 spectra obtained during flash experiments succeedingly run after these interruptions. From this it is suggested that indeed only lower Θ_O-, Θ_{CO}-values influence the spectra. By integration of the flash spectra in Fig. 1 one can determine the total amount of CO_2 formed in the respective flash measurements. The results are shown in Figure 3. As expected, with increasing oxygen coverage the exposure of CO needed to saturate the $\int p_{CO_2}$-value increases. In addition it is seen that for a fixed Θ_O there are regions where CO is present at the surface in deficiency (low CO exposures) or in excess (high CO exposures). From a separate set of measurements the efficiency of the reaction was determined to be $\sim 40\%$ at maximum, even in those cases where CO was deficient, more than half of the CO molecules desorb and do not react.

3.4. Stationary Reaction

The steady state reaction was investigated with constant oxygen and CO partial pressures ranging from 10^{-8} to 10^{-7} torr. Figure 4 shows the steady-state rate of CO_2 formation as a function of the sample temperature T for one specific set of p_{O_2}, p_{CO}. Within the measured range, no significant change of the relative rate as a function of T occurs upon variation of p_{O_2}, p_{CO}. By monitoring simultaneously the peak height of the carbon Auger signal, the CO coverage Θ_{CO} during the reaction was determined. Its temperature dependence is displayed in Figure 4. The correlation of Θ_{CO} and p_{CO_2} clearly shows the inhibitor effect arising from adsorbed CO. Without further assumptions a decision about the ruling reaction mechanism leading to the reaction rate dependence shown in Fig. 4 cannot be made.

4. Discussion

In order to establish a basis to explain the stationary reaction rate one has to take the foll-

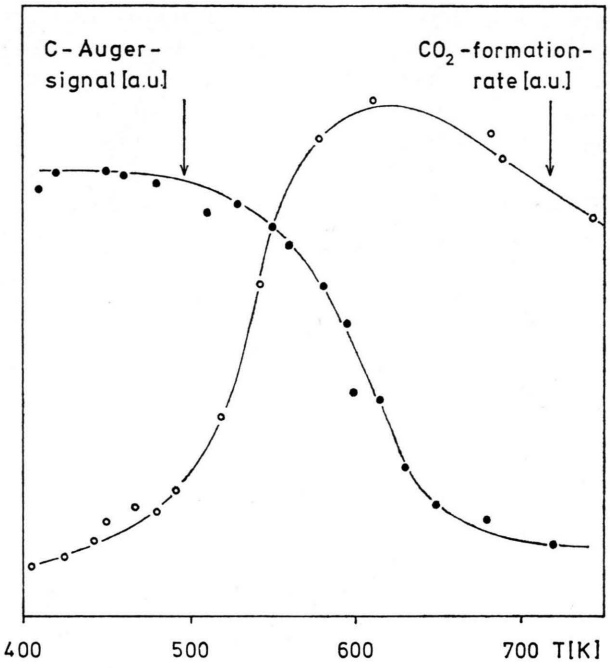

Fig. 4. Stationary CO_2 formation rate using constant oxygen and CO partial pressures as a function of temperature (left scale). CO coverage as determined from AES established during this reaction (right scale).

ing microscopic reaction steps into account:

$$CO_{gas} \xrightarrow{k_1} CO_{ad}\,, \tag{1}$$

$$CO_{ad} \xrightarrow{k_{-1}} CO_{gas}\,, \tag{2}$$

$$O_{2gas} \xrightarrow{k_2} 2\,O_{ad}\,, \tag{3}$$

$$2\,O_{ad} \xrightarrow{k_{-2}} O_{2gas}\,, \tag{4}$$

$$CO_{ad} + O_{ad} \xrightarrow{k_3} CO_{2ad} \xrightarrow{k_4} CO_{2gas}\,, \tag{5}$$

$$CO_{gas} + O_{ad} \xrightarrow{k_5} CO_{2,ad} \xrightarrow{k_4} CO_{2,gas}\,, \tag{6}$$

Step (1) is determined by the CO pressure and the sticking coefficient $s_{CO}(\Theta_{CO}, \Theta_O, T)$. Step (2) involves the activation energy for desorption via $k_{-1} = \nu_0 \exp\{-E_{des}(\Theta_{CO}, \Theta_O)/RT\}$. Step (3) is ruled by the sticking coefficient $s_O(\Theta_{CO}, \Theta_O, T)$ and the oxygen partial pressure. Step (4) can be neglected as within the temperature range under investigation the oxygen desorption is negligible. Step (5) is the LH reaction step, in which for completeliness the product desorption has been included. As the adsorption energy of CO_2 is less than 10 kcal/mol, the desorption can not be a rate determining step any may be neglected. Step (6) is the ER reaction. The sticking coefficients s_{CO} and s_O as well as E_{des} have been determined from adsorption and flash desorption experiments, thus k_1, k_{-1} and k_2 are known.

In order to get $k_3 = \nu_{LH} \exp\{-E_{LH}/RT\}$ the desorption — or more precisely: CO_2 formation spectra of Fig. 1 were evaluated using a "second order plot", as it is commonly used to get the activation energy from second order desorption spectra [7].

As can be seen in Fig. 5, precovering the surface with $\Theta_O = 0.25$ which means oxygen excess for all CO exposures leads to almost constant values of $N_p T_p^2/\beta$, N_p being the total number of adsorbed particles at the desorption peak maximum, T_p the temperature at peak maximum and β the heating rate. With $\Theta_O = 0.03$ two regions of CO excess and

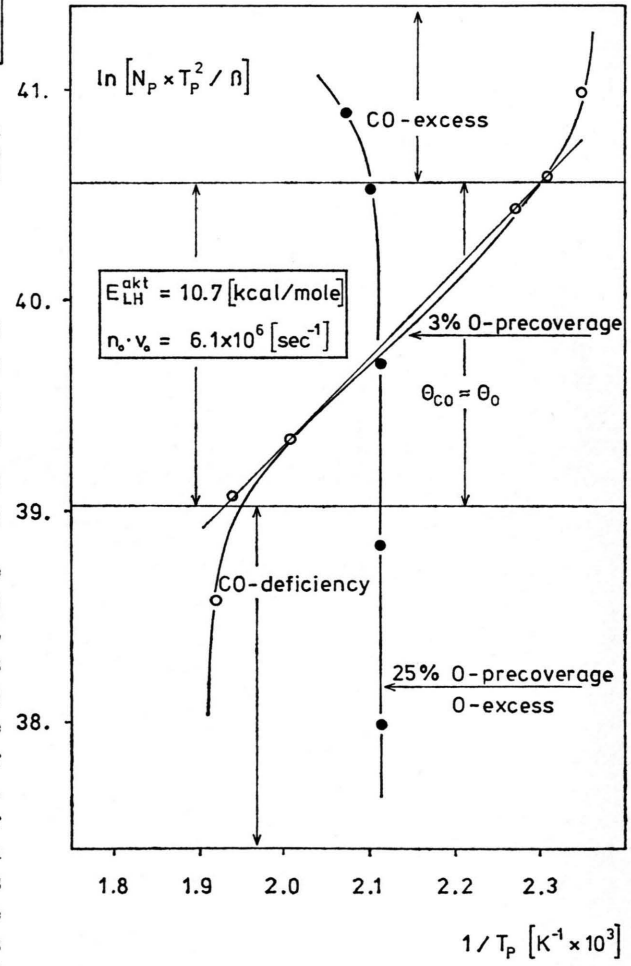

Fig. 5. Second order plots for instationary CO_2 formation spectra. See text.

deficiency are separated by a region where $\Theta_O \approx \Theta_{CO}$. A linear dependence of $\ln N_p T_p^2/\beta$ vs. $1/T_p$ is present in this region suggesting a second order process. An activation energy of 10.7 kcal/mole and a frequency factor of $6.1 \cdot 10^6$ sec^{-1} can be concluded from the linear part.

The behaviour of the peak positions in Fig. 1 can be understood with a simple model.

The appropriate reaction chain can be written as

$$CO_{ad} + O_{ad} \overset{K}{\rightleftarrows} [O{-}CO]_{ad} \xrightarrow{k_R} CO_{2ad} \xrightarrow{k_{des}} CO_{2gas}.$$

From this it follows

$$p_{CO_2} = \frac{dn_{CO_2\,gas}}{dt} = k_R^0 \quad \exp\left\{-\frac{E_R}{RT}\right\} K\, n_{CO_{ad}}\, n_{O_{ad}}$$

having used the stationary condition

$$dn_{CO_2\,ad}/dt \approx 0\,.$$

At peak maximum, $T = T_p$, the condition $dp_{CO_2}/dt = 0$, has to be fulfilled, which leads to

$$\exp\{E_R/RT_p\} = \frac{R}{E_R} K \frac{k_R^0 T_p^2}{\beta} (n_{CO_{ad}}^{T_p} + n_{O_{ad}}^{T_p}),$$

$$\beta = dT/dt\,.$$

From this equation it is easily seen, that an excess concentration of CO or O results in a constant peak temperature T_p. If $n_{CO_{ad}} \approx n_{O_{ad}}$ there should be a linear relation between $\log N_p T_p^2/\beta$ and $1/T_p$ which is in fact observed. However, the activation energy calculated from Fig. 5 is the activation energy E_R for the LH mechanism, the frequency factor giving the respective prefactor of the exponential function within the coverage region under investigation.

The reaction schemes (2)–(6) listed above have in principle to be used to get differential equations determining $\Theta_O(t)$, $\Theta_{CO}(t)$. As no functional expressions but only measured data are available for $s_{CO}(\Theta_O, \Theta_{CO})$, $s_O(\Theta_O, \Theta_{CO})$, $E_{des}^O(\Theta_O)$ these coupled differential equations are almost impossible to be solved analytically.

Instead, a different approach was used to calculate the reaction rate $dn_{CO_2g}/dt = p_{CO_2}$ by means of a computer simulation. This was done by computing each of the involved reation steps for small time intervals of 10^{-3} sec succeedingly. By repetitively proceeding through all steps the equilibrium values of Θ_{CO}, Θ_O and p_{CO_2} were approached. For each temperature up to 10^9 repetitions were needed to establish equilibrium. In detail, the following parameters were included: $p_{O_2} = p_{CO} = 1.1 \cdot 10^{-7}$ torr, $T_{gas} = 300$ K, density of adsorption sites at the surface: $1.56 \cdot 10^{15}$ cm^{-2}, prefactor of CO desorption: 10^{13} sec^{-1}, prefactor of LH-reaction $6.1 \cdot 10^6$ sec^{-1}, $E_{akt}^{LH} = 10.7$ kcal/mole. From separate measurements experimental data were used for:

$$s_{CO}(\Theta_{CO}, \Theta_O), \quad E_{des}^{CO}(\Theta_{CO}),$$

$$s_O(\Theta_O, \Theta_{CO}), \quad E_{des}^{O}(\Theta_O).$$

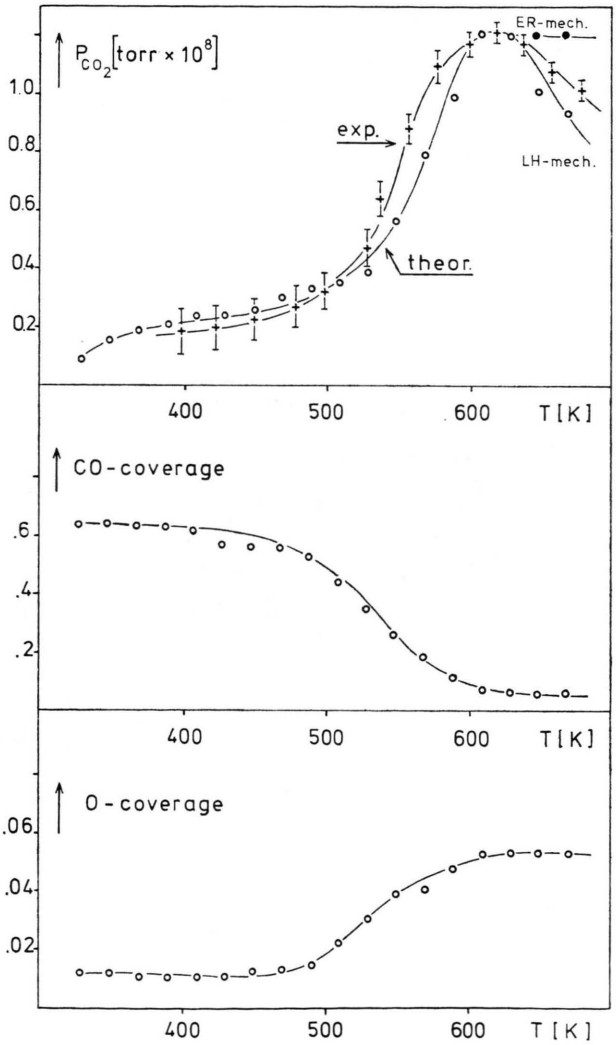

Fig. 6. Theoretical and experimental stationary CO_2 formation rate as a function of temperature (upper part). Theoretical oxygen and CO coverages established during reaction (lower part).

The reaction step (4) was neglected, the activation energy for ER reaction, step (6) was neglected, i.e.

$$k_5 = p_{CO}(2\pi m kT)^{-1/2} \exp\{-E_{akt}^{ER}/RT\}, E_{akt}^{ER} \approx 0.$$

The result of this calculation is shown in Figure 6.

It should be noted, that the absolute scale of p_{CO_2} was determined using the characteristic pumping speed of the vacuum system; no scale fitting has been applied to the diagram.

It is seen that the theoretical CO_2 reaction rate agrees very well with the experimental curve taken from Fig. 5, if only the operation of an LH mechanism is assumed. Adding the operation of ER reaction to the calculation the results are in an obvious disagreement above 600 K. Thus the ER mechanism is ruled out. The temperature dependence of the reaction rate is most easily understood from the oxygen and CO coverages established at different temperatures during the reaction. Up to 500 K the surface is almost completely covered with adsorbed CO, $\Theta_{CO} \geqq 0.5$ whereas the oxygen coverage Θ_O remains below ~ 0.01. As the dissociation of oxygen supplied by the adsorption process is required to initialize the CO_2 formation, the CO_2 partial pressure is low. Between 500 K and 600 K the CO coverage drops to less than 0.1, thus enabling oxygen adsorption. In this temperature range the oxygen coverage increases to ~ 0.06. By comparison with Fig. 4 it is seen that the calculated drop of Θ_{CO} is proved experimentally.

Upon these drastic changes of Θ_{CO} and Θ_O even the CO_2 formation rate undergoes its biggest change within the temperature range under investigation. Between 500 K and 600 K the rate increases by a factor of 4, indeed resembling the experimental data.

Above 600 K the calculated rate is different with and without inclusion of the ER mechanism. Taking the operation of an ER mechanism into account results in an almost constant CO_2 formation rate. This is a simple consequence of the rate law governing this mechanism, depending principally on the CO partial pressure and oxygen coverage. The assumption $E_{akt}^{ER} = 0$ made for simplicity does not effect the calculated results, as even accounting for a value of $E_{akt}^{ER} \neq 0$ (within a meaningfull range up to ~ 10 kcal/mole) no change of the rate has been observed. This is comprehensible regarding the temperature at which this reaction is assumed to be important.

The constant CO_2 formation rate above 600 K is in complete disagreement with the experimental data, which suggest a decrease of the rate. This behaviour is predicted from the calculations when only the operation of the LH mechanism is assumed. The origin of the decrease can be traced back to the kinetics of steps (2) and (5) listed above. It is seen from Fig. 5 that the coverages Θ_{CO} and Θ_O are almost constant in the temperature range in which the rate drops significantly. Thus the prerequisite for the LH reaction, adsorbed CO and oxygen, is fulfilled. On the other hand, the kinetics of steps (2) and (5) start to be competitive as the desorption step may be faster than the reaction step. With increasing temperature the balance between desorption and reaction tends to favour the desorption step, from which a decrease of the reaction rate is produced.

It should be noted that within the temperature region scanned by Fig. 5, the oxygen coverage is very small, below 0.06. At low temperatures this is caused by the inhibitor effect of adsorbed CO, at high temperatures this is a consequence of the small sticking coefficient of oxygen in conjunction with the reactive oxygen removal.

In conclusion, from a comparison of experimental and theoretical data it follows that the ER reaction mechanism cannot be operating in the CO-oxidation reaction at Ir(111) surfaces. As experimental stationary CO_2 formation results with other platinum metal surfaces exhibit similar features as observed with Ir(111), it is suggested that the ER mechanism is not acting in the CO oxidation at these metals.

5. Conclusions

a) The activation energy for the LH reaction $CO_{ad} + O_{ad} \rightarrow CO_2$ at Ir(111) surfaces is determined to be 10.7 kcal/mole.

b) A computer simulation of the stationary CO_2 formation leads to different reaction rates with and without inclusion of the ER reaction mechanism.

c) The experimentally determined reaction rate can only be explained when no ER mechanism is taken into account.

[1] a) G. Ertl and P. Rau, Surf. Sci. **15**, 443 (1969). b) G. Ertl and M. Neumann, Z. Phys. Chemie N.F. **90**, 127 (1974). c) T. Matsushima and J. M. White, J. Catalysis **40**, 334 (1975).
[2] a) H. P. Bonzel and R. Ku, Surf. Sci. **33**, 91 (1972). b) H. Hopster, H. Ilbach, and G. Comsa, J. Catalysis **46**, 37 (1977).
[3] a) J. Küppers, and A. Plagge, J. Vac. Sci. Techn. **13**, 259 (1976). b) V. P. Ivanov, G. K. Boreskov, U. I. Savchenko, W. F. Egelhoff, and W. H. Weinberg, J. Catalysis **48**, 269 (1977).
[4] T. E. Madey, H. A. Engelhardt, and D. Menzel, Surf. Sci. **48**, 304 (1975).
[5] a) T. Engel and G. Ertl, J. Chem. Phys. in press. b) R. L. Palmer and J. N. Smith, J. Chem. Phys. **60**, 14353 (1973).
[6] H. Conrad, G. Ertl, and J. Küppers, Surf. Sci. **76**, 323 (1978).
[7] L. R. Clavenna and L. D. Schmidt, Surf. Sci. **22**, 365 (1970).